Available online at www.sciencedirect.com
SCIENCE DIRECT®
Journal of Organometallic Chemistry 681 (2003) 51–58
Journal of Organometallic Chemistry
www.elsevier.com/locate/jorganchem

Synthesis, structural characterization and electroluminescence study of alkylgallium derivatives of thiobenzhydrazones

Yingzhong Shen [a,b,1], Hongwei Gu [a], Weijin Gu [a], Fang Yuan [a], Yu Zhu [c], Yi Pan [a,*]

[a] Department of Chemistry, School of Chemistry and Chemical Engineering, Nanjing University, Nanjing 210093, China
[b] Technische Universität Chemnitz, Institut für Chemie, Straße der Nationen 62, D-09111 Chemnitz, Germany
[c] Analysis Center of Zhengzhou University, Zhengzhou 450052, China

Received 28 April 2003; received in revised form 23 May 2003; accepted 23 May 2003

Abstract

Six dimethylgallium complexes of type Me_2GaL [L = *N*-benzylidenethiobenzahydrazonato (**1**), *N*-(4-methoxy)benzylidenethiobenzahydrazonato (**2**), *N*-(3,4-dimethoxy)benzylidenethiobenzahydrazonato (**3**), *N*-(4-*N*,*N*-dimethylamino)benzylidenethiobenzahydrazonato (**4**), *N*-(2-naphthyl)methylenethiobenzahydrazonato (**5**) and *N*-(9-anthryl)methylenethiobenzahydrazonato (**6**)] have been synthesized by reaction of trimethylgallium with appropriate *N*-arylmethylenethiobenzahydrazones. The complexes obtained have been characterized by elemental analysis, ^{1}H-NMR, IR and mass spectroscopy. Structure of **2** has been determined by X-ray single-crystal analysis, in which Ga atom is four-coordinated. Compounds **2**–**4** emit blue colors at $\lambda_{max} = 432$–479 nm when irradiated by UV light. The electroluminescent (EL) properties of **2**, **3** and **4** were examined by fabricating EL devices using **2**, **3** and **4** as emitter, respectively. The EL bands are located in the blue region (451, 454 and 479 nm for complexes **2**, **3** and **4**, respectively).

Keywords: Trialkylgallium; Thiobenzhydrazone; X-ray crystallography; Electroluminescence

1. Introduction

Organic electroluminescent devices (OLEDs) have attracted much interest due to their potential emission of all colors (from blue to red) and their possible applications in large-area displays since Tang et al. [1,2] reported the bright OLED at low voltages. Blue luminescent compounds are among the most sought-after materials by scientists because of their potential applications in full-color electroluminescent (EL) displays [3–7]. Unlike the other two key components, red and green, which are readily available, useful blue luminescent materials for OLED displays are still scarce. Most of the reported EL organic compounds in OLED are either aromatic molecules or organic polymers [8–11]. Although quite a few metallic complexes such as 8-hydroxyquinoline or azomethine-coordinated Al(III), Zn(II) or Be(II) complexes have been used as OLED-emitting material [12–15] and some of them have been reported to have blue photoluminescent characteristics [16–18], few organogallium compound-based EL diodes have been reported up to our knowledge [19,20]. So development of various EL materials and study of relationship between structure and electroluminescence property are in great need. Recently, we reported a bluish-green variable light-emitting diode based on an organicgallium complex [19]. In this report, the synthesis and characterization of various dimethyl(*N*-arylmethylenethiobenzahydrazonato)gallium complexes are described. A crystal structure of **2** has been determined by X-ray analysis. Both the photoluminescent and EL properties of complexes **2**, **3** and **4** have been measured and discussed.

* Corresponding author. Tel.: +86-25-3592485; fax: +86-25-3317761.
E-mail addresses: yingzhong.shen@chemie.tu-chemnitz.de (Y. Shen), mochemnu@public1.ptt.js.cn (Y. Pan).
[1] Tel.: +49-371-531-1381; fax: +49-371-531-1200.

0022-328X/03/$ - see front matter © 2003 Published by Elsevier B.V.
doi:10.1016/S0022-328X(03)00530-8

2. Results and discussion

2.1. Synthesis and characterization

Reactions of thiobenzhydrazones, which were obtained by the condensation of thiobenzoylhydrazide with benzaldehyde, 4-methoxybenzaldehyde, 3,4-dimethoxybenzaldehyde, 4-*N*,*N*-dimethylaminobenzaldehyde, 2-naphthaldehyde and 9-anthraldehyde, respectively, with trimethylgallium proceeded smoothly at room temperature. Due to keto-enol tautomerism, the gallium atom is believed to bond directly to the sulfur atom of the ligands. The nitrogen atom in the enaminic group will coordinate to the gallium atom too as shown in Scheme 1. The complexes were isolated as yellow or brown solid in almost quantitative yields. Although trimethylgallium is extremely moisture and oxygen-sensitive, the complexes obtained are fairly stable on exposure to air. Compounds **1**–**6** could be left in ambient atmosphere for months without obvious decomposition. The complexes are nearly insoluble in cold saturated hydrocarbons such as pentane or petroleum and fairly soluble in unsaturated hydrocarbons such as benzene or toluene. All products obtained gave satisfactory elemental analysis results and have been characterized with ^{1}H-NMR, IR and mass spectroscopy, respectively.

In the IR spectra of the complexes, absence of N–H stretch vibration absorption verifies the reaction of the active hydrogen atom of the ligands with trimethylgallium. It is also confirmed by the absence of nitrogen-bonded proton signals in the ^{1}H-NMR spectra of complexes. In IR spectra, C–H stretch vibrations of the gallium-bonded methyl groups are visible in the region between 2900 and 2950 cm^{-1}, although they are weak. Proton signals on the gallium-bonded methyl groups in ^{1}H-NMR move downfield compared with those in trimethylgallium, demonstrating the electron-withdrawing nature of the ligands. M^+ peak of complex **2** was observed in its mass spectrum. Although M^+ peaks of other complexes were not visible, fragments of eliminating one or two methyl groups appeared in their mass spectra with fairly high intensity. Relative peak intensities of the gallium-containing species agree well with the isotopic distribution of the gallium atoms [^{69}Ga (ca. 60%); ^{71}Ga (ca. 40%)].

2.2. Solid-state structure of *2*

A single-crystal structure of compound **2** is shown in Fig. 1 with selected bond lengths and angles listed in Table 2. Compound **2** exists as a monomer, although most of the dimethylgallium alkoxides or phenoxides occur usually as dimers [21–23]. This may be due to the strong coordination capability of the enaminic nitrogen. The geometry of Ga atom is in distorted tetrahedral. Both S and the enaminic N atoms bond to the gallium atom as expected. It is interesting to see, however, that the angle of S–Ga–N(2) is only 84.51(12)°, which is much smaller than that expected for a tetrahedral configuration. This may be caused by the strain in the five-membered ring Ga S C(7) N(1) N(2). The angle of

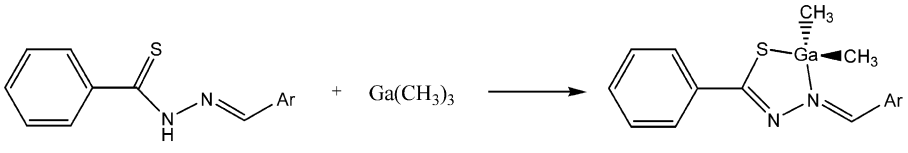

1 - 6

Compd. No.	Ar-
1	phenyl
2	4-methoxylphenyl
3	3,4-dimethoxylphenyl
4	4-*N*,*N*-dimethylaminophenyl
5	2-naphthyl
6	9-anthryl

Scheme 1.

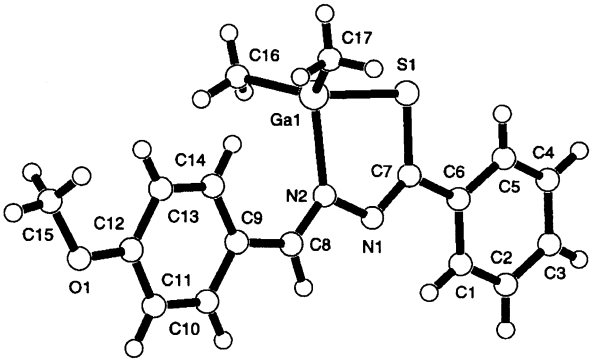

Fig. 1. Molecular structure of **2**, showing 50% probability displacement ellipsoids.

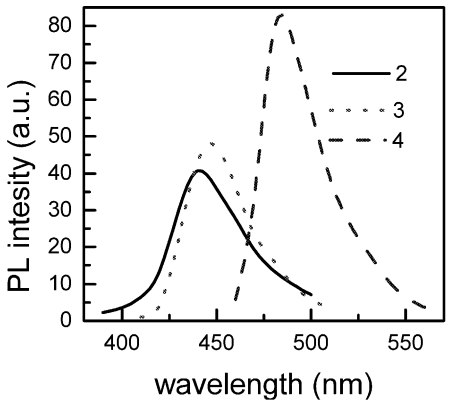

Fig. 3. Photoluminescence spectra of **2**, **3** and **4** in solution.

C(16)–Ga–C(17) is 123.9(3)°, reflecting that the steric hindrance between the two methyl groups is much larger than that of N or S atoms. The three rings of the complex is nearly coplanar, gallium-bonded methyl is perpendicular approximately to the plane. S–Ga distance (2.2874(18) Å) is shorter, while the N–Ga distance (2.098(4) Å) is longer than those reported in dimethyl[2-(phenylamino)methylene-3(2*H*)benzofuranthionato-N]gallium (S–Ga, 2.321(2) Å; N–Ga, 2.055(5) Å) [24]. This agrees well with the fact of covalent S–Ga and coordinative N–Ga bond nature. It is very interesting to see from the unit cell, shown in Fig. 2, that the two molecules of complex overlap each other. Although the distance between them is rather far, there should have some weak π–π interactions between the phenyl rings of the molecule.

2.3. Photoluminescence studies

Photoluminescence emission spectra of complexes **2**–**4** were measured in solution (Fig. 3) as well as in solid state (Fig. 4). Seen from Fig. 3 the emission bands are located in the blue region. When irradiated by UV light, the maximum emission is at $\lambda = 432$ nm with an intensity of 40.7 au for complex **2**, 446 nm with an intensity of 47.5 au for complex **3** and 479 nm with an intensity of 78.6 au for complex **4**. The PL spectra of powder samples of **2**–**4** (Fig. 4) match those in solution. The fact that compounds **2**–**4** have a similar emission band in solution and solid indicates that the luminescence observed in these compounds is a molecular property, attributable to a π–π* transition of the *N*-arylmethylenethiobenzahydrazones. As shown in the spectra (Figs. 3 and 4), there is a dramatic red-shift of emission energy of complex **4** comparing to those of the complexes **2** and **3**, attributing to the stronger electron-repelling capability of dimethylamino substitute, which increases the HOMO level and hence decreases the HOMO and LUMO gap. Complexes **2**–**4** are three rare examples of blue luminescent material of organogallium complexes. The photoluminescence of compounds **2**–**4** is in sharp contrast to those of the free ligands, which have weak emission. The strong blue luminescence observed may be attributed to the coordination or bridging of the ligands to the gallium center, which increases the rigidity of the ligand and reduces the loss of energy via un-radiation pathway, thus enhancing the $\pi^* \rightarrow \pi$ irradiation probability. Different complexes exhibit different photoluminescence characteristics illustrating that different substitutes exert different effects on photoluminescence.

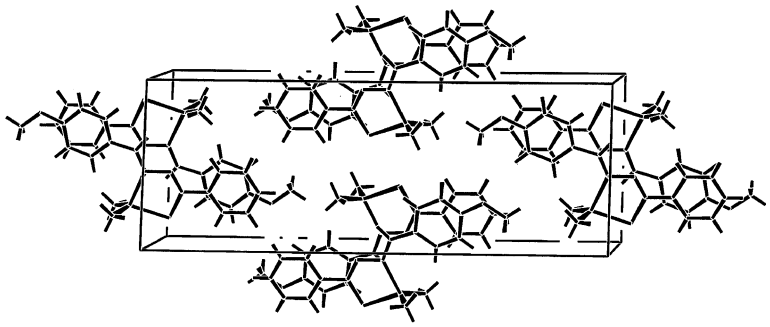

Fig. 2. Unit cell of **2**.

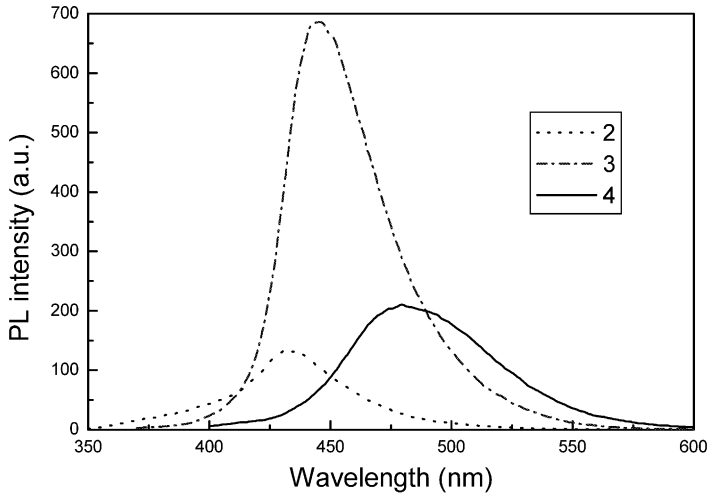

Fig. 4. Photoluminescence spectra of **2**, **3** and **4** in solid state.

2.4. Electroluminescence study

The electroluminescence device structure is shown in Fig. 5. The gallium complexes were used as light-emitting layer. The complexes were dissolved in dichloromethane. The device was prepared on patterned indium-tin-oxide (ITO) coated on glass substrate, which was cleaned by ultrasonic in a mixture of isopropanol and water (1:1) and degreased in toluene vapor, with a sheet resistance of about 80 Ω/sq. Due to the poor film-forming properties of the complexes, a very small quantity of polymethylmethacrylate (PMMA), which is inert to light and electricity, was used to improve the film-forming properties by mixing it with the organo-gallium complexes. A device structure of ITO/emissive layer/Al was employed. High-quality film can be obtained by spin-cast of PMMA and gallium complexes mixture dissolved in dichloromethane. An electron-injecting electrode Al was deposited on top by vacuum evaporation at pressure below 2×10^{-5} Torr with a deposition rate of 10–15 Å s^{-1}. The emitting area was 2×3 mm^2. The luminance of the EL devices was measured with a Perkin–Elmer LS 50B fluorescence spectrophotometer. Meanwhile, the current density was recorded with a digital multimeter. All measurements were carried out at room temperature under DC bias conditions.

The current–voltage relationship of the EL device is shown in Fig. 6. The forward bias current can be obtained when the ITO electrode is positively biased

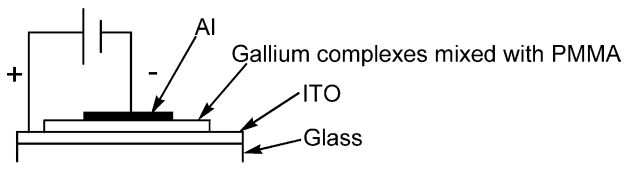

Fig. 5. Configuration of EL device.

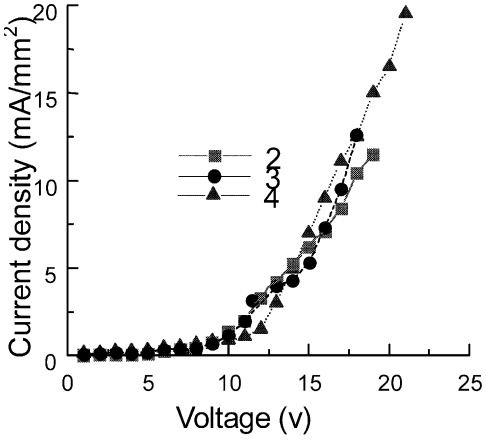

Fig. 6. The relationship of current density and voltage of EL cell with the emitter of complexes **2**, **3** and **4**.

and the Al electrode negatively. Current density increasing rate is very low at low voltage. It increases from 0.04 to 0.22 mA mm^{-2} for complex **2**, from 0.04 to 0.33 mA mm^{-2} for complex **3** and from 0.09 to 0.4 mA mm^{-2} for complex **4** when the bias voltage increases from 1 to 6 V. The current density increasing rate becomes larger when the voltage is over 8 V (from 0.4 to 12.6 mA mm^{-2} when the bias voltage increases from 8 to 18 V for complex **3** and from 0.62 to 19.5 mA mm^{-2} when the bias voltage increases from 8 to 21 V for complex **4**). The current density increasing rate for complex **2**, however, is lower than those of **3** and **4** (from 0.04 to 11.5 mA mm^{-2} when the bias voltage increases from 1 to 20 V).

The EL emission intensity–voltage as well as the EL emission intensity–current density relationships of the EL devices has been measured and are shown in Figs. 7 and 8, respectively. Seen from Fig. 7 the light output of the EL devices is increased with the input voltage in the

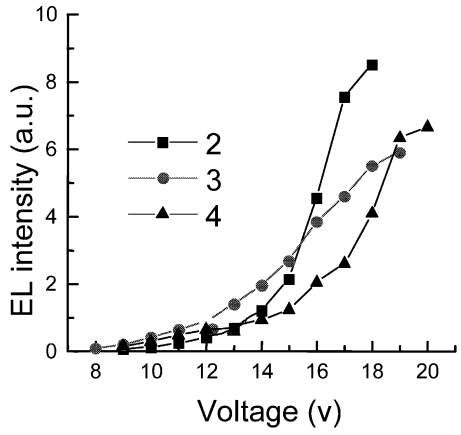

Fig. 7. EL intensity–voltage curve of EL cell with the emitter of complexes **2**, **3** and **4**.

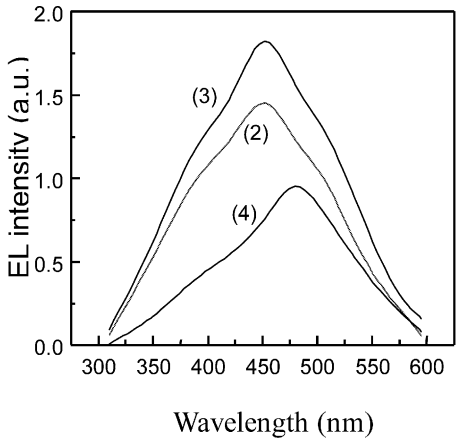

Fig. 9. Electroluminescence spectra of EL cell with the emitter of complexes **2**, **3** and **4**.

range 9–18 V (**2**), 8–19 V (**3**) and 9–20 V (**4**). The emission intensity increases with increasing forward bias voltage. The EL intensity-increasing rate for complex **3** is larger than those of **2** and **4** when voltage increases from 8 to 15 V. When applied voltage is larger than 15 V, however, the EL intensity-increasing rate of **2** is larger than those of **3** and **4**. This implies that different substitutes on the complexes have different effects on the electroluminescence properties in different voltage. The driving voltages of the present diodes (8–9 V) are much lower than that of tri(1,3-diphenyl-1,3-propanediono)monophenathroline Eu(III) (driving voltage is 25 V) [25] and is similar to tris(8-hydroxyquinolinato)aluminum (below 10 V) [26].

The EL luminescence spectra of the EL devices are shown in Fig. 9. Their EL bands are all located in the blue region. The EL emission maxima are 451, 454 and 479 nm with the intensities of 1.45, 1.84 and 0.94 au for complexes **2**, **3** and **4**, respectively. As shown in Fig. 9, the emission maxima of the devices are related to the substitutes on the phenyl ring. The emission bands are similar to those of the photoluminescence emission spectra. This illustrates that the EL spectra are independent of the driving voltage and current. The result also indicates that the radiative recombination of injected electrons and holes takes place in the gallium complexes. The role of gallium atom in the blue luminescence of complex is considered to be twofold. First, the formation of covalent bond between the gallium and the sulfur atom and of the donor–acceptor bond between the gallium and the nitrogen atom which may contribute to the perturbation of the π energy level, thus change the $\pi^* \rightarrow \pi$ transition energy of the ligand. The second, the binding of thiobenzhydrazone ligands to the gallium atom increases the rigidity of the ligand, thus reducing the loss of energy via un-radiation vibration motions and increasing the emission effi-

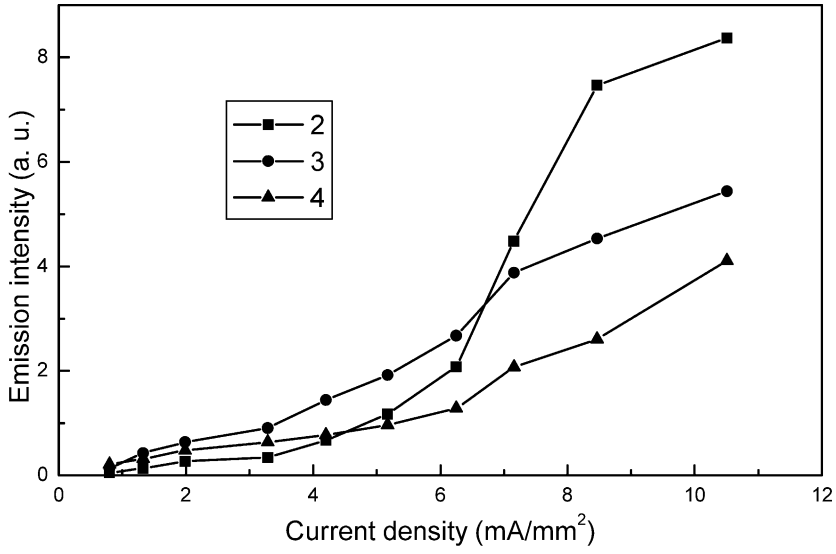

Fig. 8. EL intensity–current curve of EL cell with the emitter of complexes **2**, **3** and **4**.

ciency. The effect of substitutes on ligands as well as the different alkyl substitutes of gallium atom on electroluminescence is being investigated in detail in our laboratory.

3. Experimental

3.1. General procedure

All reactions were performed in a glove box under purified nitrogen. The solvents were refluxed with sodium benzophenone and distilled under nitrogen prior to use. Thiobenzhydrazones were prepared by condensation of thiobenzhydrazide with benzaldehyde, 4-methoxybenzaldehyde, 3,4-dimethoxy-benzaldehyde, 4-*N*,*N*-dimethylaminobenzaldehyde, 2-naphthaldehyde and 9-anthraldehyde, respectively. Trimethylgallium was provided by the National 863 Program Advanced Material MO Precursors R&D Center of Nanjing University. ^{1}H-NMR spectra were recorded on a Bruker ARX-300 spectrometer with TMS as internal standard. Infrared spectra were collected on a Shimadzu IR 408 instrument in KBr pellets. Mass spectra were measured on a VG-ZAB-HS spectrometer (electron impact ionization). Elemental analyses were performed on a Perkin–Elmer 240 C elemental analyzer. Luminescence spectra were measured on a Perkin–Elmer LS 50B fluorescence spectrophotometer. Melting points were observed in sealed capillaries and were uncorrected.

3.2. Preparation of dimethyl[benzylidenethiobenzhydrazonato]gallium (*1*)

A solution of trimethylgallium (0.24 g, 2.1 mmol) in 10 ml of cyclohexane was added dropwise over a period of 10 min with stirring to a solution of benzylidenethiobenzhydrazone (0.48 g, 2 mmol) in a mixture of 10 ml cyclohexane and 2 ml benzene. After the mixture was stirred for an additional 5 min at room temperature, volatiles were removed in vacuo and the yellow powder residue was recrystallized from cyclohexane/benzene solution, giving **1** (0.68 g) in a yield of 86%. m.p.: 76–78 °C. Anal. Calcd. for $C_{16}H_{17}N_2SGa$: C, 56.68; H, 5.05; N, 8.26. Found: C, 56.34; H, 4.93; N, 7.96%. ^{1}H-NMR data (δ ppm in C_6D_6): 6.9–8.3 (m, 10H, Ph–*H*), 8.6 (s, 1H, Ph–C*H*=N), −0.16 (s, 6 H, Ga*Me*$_2$). IR data (cm^{-1}): 3050 (w), 2999 (w), 2948 (w), 1624 (vs), 1574 (vs), 1492 (w), 1446 (m), 1210 (w), 1072 (w), 956 (m), 857 (w), 752 (vs), 691 (vs), 497 (M). MS data: 209 (8.53%), 208 (57.67%), 207 (52.97%), 181 (10.30%), 179.9 (18.32%), 177.9 (4.28%), 165 (4.05%), 131 (16.35%), 105 (22.10%), 104 (100%), 103 (24.02%), 102 (9.37%), 91 (10.28%), 90 (16.33%), 89 (23.37%), 82.6 (13.13%), 78 (21.4%), 77 (93.15%), 71 (2.47%), 69 (1.02%).

3.3. Preparation of dimethyl[(4-methoxy)benzylidenethiobenzhydrazonato]gallium (*2*)

Prepared in the same manner as described for **1** from (4-methoxy)benzylidenethiobenzhydrazone (0.58 g, 2 mmol) and trimethylgallium (0.24 g, 2.1 mmol). Compound **2** was isolated as yellow crystal. Yield: 0.65 g (88%). m.p.: 100–102 °C. Anal. Calcd. for $C_{17}H_{19}N_2OSGa$: C, 55.32; H, 5.20; N, 7.59. Found: C, 54.13; H, 5.02; N, 7.27%. ^{1}H-NMR data (δ ppm in C_6D_6): 6.9–8.3 (m, 8H, Ph–H), 8.6 (s, 1H, Ph–C*H*=N), −0.15 (s, 6H, Ga*Me*$_2$). IR data (cm^{-1}): 3085 (w), 2964 (w), 2934 (w), 2836 (W), 1591 (vs), 1577 (vs), 1511 (VS), 1485 (s), 1267 (S), 1175 (VS), 1024 (m), 936 (m), 829 (m), 769 (M), 691 (m), 579 (M). MS data: 371 (20.7%), 369 (28.15%), 355 (26.23%), 353 (30.77%), 291 (12.85%), 271.3 (21.7%), 270.2 (14.4%), 269.3 (25.6%), 237.2 (15.72%), 135.1 (11.2%), 134.1 (100%), 131 (21.8%), 121.1 (22.2%), 119 (15.2%), 107 (10.7%), 104 (18.42%), 101 (23.9%), 99 (30.1%), 91 (56.1%), 90 (10.35%), 77 (18.5%), 73 (26.3%), 71 (12.2%), 69 (15.45%).

3.4. Preparation of dimethyl[(3,4-dimethoxy)benzylidenethiobenzhydrazonato]gallium (*3*)

Complex **3** can be synthesized in the same manner as **1** (see above). Thus, (3,4-dimethoxy)benzylidenethiobenzhydrazone (0.6 g, 2 mmol) is treated with trimethylgallium (0.24 g, 2.1 mmol). After appropriate work-up, complex **3** can be isolated as a yellow solid. Yield: 0.65 g (82%). m.p.: 158–160 °C. Anal. Calcd. for $C_{18}H_{21}N_2O_2SGa$: C, 54.16; H, 5.30; N, 7.02. Found: C, 54.05; H, 5.15; N, 6.84%. ^{1}H-NMR data (δ ppm in C_6D_6): 6.98–7.77 (m, 8H, Ph–H), 8.5 (s, 1H, Ph–C*H*=N), (s, 6H, –OCH_3), −0.23 (s, 6H, Ga*Me*$_2$). IR data (cm^{-1}): 3049 (w), 2940 (m), 2862 (m), 1590 (m), 1479 (vs), 1436 (m), 1229 (m), 939 (m), 893 (m), 744 (s), 697 (m), 649 (w). MS data: 386 (15.7%), 385 (76.2%), 384 (20.8%), 383 (100%), 299 (1.04%), 298 (2.34%), 164 (11.8%), 122 (1.05%), 121 (4.25%), 119 (2.01%), 103 (4.71%), 101 (1.5%), 99 (2.48%), 77 (3.52%), 71 (1.95%), 69 (3.64%).

3.5. Preparation of dimethyl[(4-*N*,*N*-dimethylamino)benzylidenethiobenzhydrazonato]gallium (*4*)

Prepared in the same manner as described for **1** from (4-*N*,*N*-dimethylamino)-benzylidenethiobenzhydrazone (0.57 g, 2 mmol) and trimethylgallium (0.24 g, 2.1 mmol). The compound was isolated as yellow crystal after recrystallization from benzene. Yield: 0.68 g (90%). m.p.: 164–165 °C. Anal. Calcd. for $C_{18}H_{22}N_3SGa$: C, 56.75; H, 5.80; N, 11.00. Found: C, 56.32; H, 5.26; N, 10.72%. ^{1}H-NMR data (δ ppm in C_6D_6): 6.46–8.21 (m, 9H, Ph–H), 8.3 (s, 1H, Ph–C*H*=N), −0.06 (s, 6H,

GaMe_2). IR data (cm^{-1}): 3087 (w), 3049 (w), 2949 (w), 2906 (w), 1616.7 (m), 1574 (vs), 1528 (s), 1479.9 (s), 1439 (m), 1377 (s), 1182 (s), 931 (s), 816 (m), 755 (m), 678 (w), 576 (w). MS data: 370 (5%), 369 (13.47%), 368 (70.47%), 367 (20.77%), 366 (92.55%), 352 (0.84%), 282 (2.24%), 281 (5.33%), 223 (1.98%), 221 (1.29%), 184 (1.44%), 183 (3.01%), 177 (2.74%), 148 (14.69%), 147 (100%), 146 (10.9%), 145 (21.22%), 132 (5.66%), 131 (11.33%), 129 (2.38%), 121 (11.36%), 120 (13.73%), 119 (11.28%), 105 (10.83%), 104 (13.23%), 103 (23.15%), 102 (2.9%), 101 (6.5%), 99 (9.42%), 77 (17.78%), 76 (7.68%), 71 (14.09%), 69 (20.94%).

3.6. Preparation of dimethyl[N-(2-naphthyl)methylenethiobenzahydrazonato]gallium (5)

Prepared in the same manner as described for **1** from (2-naphthyl)methylenethiobenzhydrazone (0.58 g, 2 mmol) and trimethylgallium (0.24 g, 2.1 mmol). The compound was isolated as yellow crystal after recrystallization from benzene. Yield: 0.65 g (84%). m.p.: 164–165 °C. Anal. Calcd. for $C_{20}H_{19}N_2SGa$: C, 61.85; H, 4.93; N, 7.22. Found: C, 61.31; H, 4.48; N, 6.95%. ^{1}H-NMR data (δ ppm in C_6D_6): 6.46–8.21 (m, 9H, Ar–H), 8.3 (s, 1H, Ar–C*H*=N), −0.06 (s, 6H, GaMe_2). IR data (cm^{-1}): 3087 (w), 3049 (w), 2949 (w), 2906 (w), 1616 (m), 1574 (vs), 1528 (s), 1479 (s), 1439 (m), 1377 (s), 1182 (s), 931 (s), 816 (m), 755 (m), 678 (w), 576 (w). MS data: 372.8 (2.2%), 308 (8.79%), 307 (4.02%), 292 (4.98%), 291 (17.65%), 290 (82.39%), 289 (55.04%), 288 (84.33%), 258 (6.66%), 257 (11.73%), 186 (11.70%), 185 (30.51%), 171 (22.51%), 163 (61.78%), 155 (18.42%), 154 (64.34%), 153 (57.63%), 141 (14.74%), 140 (7.87%), 139 (15.52%), 135 (24.23%), 128 (50.18%), 127 (100%), 126 (19.41%), 121 (40.32%), 104 (55.06%), 103 (41.14%), 101 (11.38%), 91 (12.98%), 77 (48.96%), 76 (14.59%), 71 (1.42%), 69 (2.77%).

3.7. Preparation of dimethyl[(9-anthryl)methylenethiobenzahydrazonato]gallium (6)

Prepared in the same manner as described for **1** from (9-anthryl)methylenethiobenzhydrazone (0.68 g, 2 mmol) and trimethylgallium (0.24 g, 2.1 mmol). The compound was isolated as yellow crystal after recrystallization from benzene. Yield: 0.76 g (87%). m.p.: 218–220 °C. Anal. Calcd. For $C_{24}H_{21}N_2SGa$: C, 65.74; H, 4.83; N, 6.38. Found: C, 65.21; H, 4.58; N, 6.14%. ^{1}H-NMR data (δ ppm in C_6D_6): 6.46–8.21 (m, 9H, *Ar*–H), 8.3 (s, 1H, An–C*H*=N), −0.06 (s, 6H, GaMe_2). IR data (cm^{-1}): 3087 (w), 3049 (w), 2949 (w), 2906 (w), 1616 (m), 1574 (vs), 1528 (s), 1479 (s), 1439 (m), 1377 (s), 1182 (s), 931 (s), 816 (m), 755 (m), 678 (w), 576 (w). MS data: 427 (4.42%), 426 (14.78%), 425 (56.56%), 424 (21.30%), 423 (76.95%), 205 (16.47%), 204 (100%), 203 (26.69%), 177 (35.66%), 176 (17.19%), 175 (4.56%), 153 (4.39%), 151 (6.48%), 121 (5.09%), 119 (4.09%), 117 (5.80%), 71 (6.97%), 69 (10.69%).

3.8. X-ray structural analysis of complex 2

Single crystal of compound **2** was obtained by recrystallization from benzene solution. A single crystal suitable for X-ray determination was mounted in a thin-walled capillary tube in a glove box, plugged with resin, removed from the glove box, then flame sealed. Data were collected at 291.2 K on a Rigaku-RaxisIVP imaging plate area detector with graphite monochromated Mo–K_α ($\lambda = 0.71073$ Å) radiation to a maximum 2θ value 55.0°. Read out was performed in the 0.100 mm pixel mode. The data were corrected for Lorentz and polarization effects during data reduction. A correction for secondary extinction was applied (coefficient = 0.0056(19)). A total of 2854 reflections were collected. The structure was solved by direct

Table 1
Crystal data, collection parameters and refinements for $C_{17}H_{19}N_2OSGa$ (**2**)

Formula	$C_{17}H_{19}N_2OSGa$
Formula weight	369.12
Crystal colour, habit	yellow, prismatic
Crystal dimensions (mm^3)	0.30 × 0.30 × 0.20
Crystal system	monoclinic
Unit cell dimensions	
a (Å)	7.4018(15)
b (Å)	25.463(5)
c (Å)	9.4617(19)
α (°)	90.00
β (°)	104.11(7)
γ (°)	90.00
V (Å^3)	1729.5(6)
Space group	$P2_1/C$
Z	4
D_{calc} (g cm^{-3})	1.418
$F(0\,0\,0)$	760
Index range (°)	$0 \le h \le 9$, $0 \le k \le 33$, $-12 \le l \le 11$
μ(Mo–K_α) (cm^{-1})	17.14
Diffractometer	Rigaku-RaxisIVP
Radiation	Mo–K_α ($\lambda = 0.72070$ Å)
Temperature (K)	291(2)
$2\theta_{max}$ (°)	54.98
No. of reflections measured	2854
Independent reflections observed (I) > 2.00 (σ(I))	2457
No. of variables	200
Correction	Lorentz polarization
$R(F)$	0.0781/0.0621
wR	0.1659/0.1559
Goodness of fit on F^2	1.120
$\Delta\rho_{max}$ (e Å^{-3})	0.890
$\Delta\rho_{min}$(e Å^{-3})	−0.421
$(\Delta/\sigma)_{max}$	0.089

Table 2
Selected interatomic bond distances (Å) and angles (°) for **2**

Bond distances			
Ga(1)–S(1)	2.2874(18)	N(1)–N(2)	1.408(6)
Ga(1)–N(2)	2.098(4)	N(1)–C(7)	1.301(7)
S(1)–C(7)	1.736(5)	N(2)–C(8)	1.305(6)
Bond angles			
S(1)–Ga(1)–N(2)	84.51(12)	S(1)–Ga(1)–C(16)	110.2(2)
S(1)–Ga(1)–C(17)	112.8(2)	N(2)–Ga(1)–C(16)	113.8(2)
N(2)–Ga(1)–C(17)	104.5(2)	C(16)–Ga(1)–C(17)	123.9(3)
Ga(1)–S(1)–C(7)	95.81(19)	N(2)–N(1)–C(7)	116.6(4)
Ga(1)–N(2)–N(1)	116.1(3)	Ga(1)–N(2)–C(8)	133.0(4)
N(1)–N(2)–C(8)	110.5(4)	S(1)–C(7)–N(1)	125.8(4)
S(1)–C(7)–C(6)	117.7(4)	N(2)–C(8)–C(9)	128.6(5)

methods [27] using Fourier technique [28]. All non-hydrogen atoms were refined anisotropically. Hydrogen atoms were included but not refined. The final cycle of full-matrix least-squares refinement was based on 2457 observed reflections $[I > 2.00\sigma(I)]$ and 200 variable parameters and converged with unweighted and weighted agreement factor of $R = \Sigma||F_o| - ||F_c||/\Sigma|F_o| = 0.0781/0.0621$, $R_w = \Sigma w(|F_o| - |F_c|^2/\Sigma w F_o^2)^{1/2} = 0.1659/0.1559$. The standard deviation of an observation of unit weight was 1.120. The maximum and minimum peaks on the final difference Fourier map corresponded to 0.890 and -0.421 e $Å^{-3}$, respectively. All calculations were performed using the TEXSAN crystallographic software package of Molecular Structure Corporation [29]. Crystallographic data and details on refinement are presented in Table 1. Selected bond distances and angles for the compound are listed in Table 2. The crystal structure of complex **2** is presented in Fig. 1.

4. Supplementary material

Crystallographic data (comprising hydrogen atom coordinates, thermal parameters and full tables of bond lengths and angles) for the structural analysis have been deposited with the Cambridge Crystallographic Center (Deposition CCDC No. 137750). Copies of this information may be obtained free of charge from The Director, CCDC, 12 Union Road, Cambridge, CB2 1EZ, UK (Fax: +44-1223-336033; e-mail: deposit@ccdc.cam.ac.uk or www: http://www.ccdc.cam.ac.uk).

Acknowledgements

We gratefully acknowledge the National Natural Science Foundation of China (Project 20072015), Science Foundation of Jiangsu Province and the 863 High Technology Program for their financial support. The research funds for Y. Pan from Qing-Lan Program of Jiangsu Province and Kua-Shi-Ji Program of Education Ministry of China are also acknowledged.

References

[1] C.W. Tang, S.A. Van Slyke, Appl. Phys. Lett. 51 (1987) 913.
[2] C.W. Tand, S.A. Van Slyke, C.H. Chen, J. Appl. Phys. 65 (1989) 3610.
[3] P.D. Rack, A. Naman, P.H. Holloway, S. Sun, R.T. Tuenge, Mater. Res. Bull. 21 (1996) 49.
[4] S.M. Sze, Physics of Semiconductor Devices, Wiley, New York, 1981.
[5] R.H. Mauch, K.O. Velthaus, B. Hüttl, U. Troppenz, R. Herrmann, SID 95 Digest, 1995, p. 720.
[6] Y. Yang, Mater. Res. Soc. Bull. 22 (1997) 31.
[7] R. Dorsinville, H. Yun, K. Kwei, Y. Okamoto, Appl. Phys. Lett. 70 (1997) 298.
[8] H.J. Brouwer, V.V. Krasnikov, A. Hilberer, G. Hadziioannou, Adv. Mater. 8 (1996) 935.
[9] Edwards, S. Blumstengel, I. Sokolik, R. Dorsinville, H. Yun, K. Kwei, Y. Okamoto, Appl. Phys. Lett. 70 (1997) 298.
[10] Y. Ohmori, M. Uchida, K. Muro, K. Yoshino, Jpn. J. Appl. Phys. 30 (1991) L1941.
[11] J.H. Burroughes, D.D.C. Bradlley, A.R. Brown, R.N. Marks, K. Mackay, R.H. Friend, P.L. Burus, A.B. Holmese, Nature 347 (1990) 539.
[12] T. Sano, M. Fujita, T. Fujii, Y. Nishio, Y. Hamada, K. Shibata, K. Kuroki, US Patent No. 5 432 014 (1995).
[13] Y. Hironaka, H. Nakamura, T. Kusumoto, US Patent No. 5 466 392 (1995).
[14] Y. Hamada, T. Sano, M. Fujta, T. Fujii, Y. Nishio, K. Shibata, Chem. Lett. (1993) 905.
[15] N. Nakamura, S. Wakabayashi, K. Miyairi, T. Fujii, Chem. Lett. (1994) 1741.
[16] J. Ashenhurst, L. Brancaleon, A. Hassan, W. Liu, H. Schmider, S.N. Wang, Q.G. Wu, Organometallics 17 (1998) 3186.
[17] W. Liu, A. Hassan, S.N. Wang, Organometallics 16 (1997) 4257.
[18] Y.Z. Shen, Y. Pan, L.Y. Wang, G. Dong, X.P. Jin, X.Y. Huang, H.W. Hu, J. Organomet. Chem. 590 (1999) 242.
[19] C.X. Xu, Y.P. Cui, Y.Z. Shen, H.W. Gu, Y. Pan, Y.K. Li, Appl. Phys. Lett. 75 (1999) 1827.
[20] L.S. Sapochak, A. Padmaperuma, N. Washton, F. Endrino, G.T. Schmett, J. Marshall, D. Fogarty, P.E. Burrows, S.R. Forrest, J. Am. Chem. Soc. 123 (2001) 6300.
[21] D.G. Hendershot, M. Barber, R. Kumar, J.P. Oliver, Organometallics 10 (1991) 3320.
[22] K.H. Thiele, E. Hecht, T. Gelbrich, U. Dumichen, J. Dumichen, J. Organomet. Chem. 89 (1997) 540.
[23] H. Schumann, M. Frick, B. Heymer, F. Girgsdies, J. Organomet. Chem. 9 (1987) 326.
[24] V.I. Bregadze, N.G. Furmanova, L.M. Golabinskaya, O.Y. Kompan, Y.T. Struchkov, J. Organomet. Chem. 1 (1980) 192.
[25] D.G. Ma, D.K. Wang, Z.Y. Hong, X.J. Zhao, X.B.J.F.S. Wang, Chin. J. Chem. 16 (1998) 1.
[26] C.W. Tang, S.A. Van Slyke, C.H. Chen, J. Appl. Phys. 65 (1989) 3610.
[27] A. Altomare, M.C. Burla, M. Camalli, M. Cascarano, C. Giacovazzo, A. Guagliardi, G. Polidori, J. Appl. Crystallogr. 27 (1994) 435.
[28] P.T. Beurskens, G. Admiraal, G. Beurskens, W.P. Bosman, R. de Gelder, R. Israel, J.M.M. Smits, The DIRDIF-94 program system, Technical Report of the Crystallography Laboratory, University of Nijmegen, the Netherlands, 1994.
[29] Crystal Structure Analysis Package, Molecular Structure Corporation, 1985 and 1992.